

Candidate super star cluster progenitor gas clouds possibly triggered by close passage to Sgr A*

S. N. Longmore,^{1,2*} J. M. D. Kruijssen,³ J. Bally,⁴ J. Ott,⁵ L. Testi,^{1,6} J. Rathborne,⁷ N. Bastian,² E. Bressert,⁷ S. Molinari,⁸ C. Battersby⁴ and A. J. Walsh⁹

¹European Southern Observatory, Karl-Schwarzschild-Strasse 2, D-85748 Garching bei München, Germany

²Astrophysics Research Institute, Liverpool John Moores University, Twelve Quays House, Egerton Wharf, Birkenhead CH41 1LD, UK

³Max-Planck Institut für Astrophysik, Karl-Schwarzschild-Strasse 1, D-85748 Garching, Germany

⁴Center for Astrophysics and Space Astronomy, University of Colorado, UCB 389, Boulder, CO 80309, USA

⁵National Radio Astronomy Observatory, PO Box 0, 1003 Lopezville Road, Socorro, NM 87801, USA

⁶INAF–Osservatorio Astrofisico di Arcetri, Largo E. Fermi 5, I-50125 Firenze, Italy

⁷CSIRO Astronomy and Space Science, Epping, Sydney, Australia

⁸INAF–Istituto Fisica Spazio Interplanetario, Via Fosso del Cavaliere 100, I-00133 Roma, Italy

⁹International Centre for Radio Astronomy Research, Curtin University, GPO Box U1987, Perth WA 6845, Australia

Accepted 2013 April 2. Received 2013 March 25; in original form 2013 February 19

ABSTRACT

Super star clusters are the end product of star formation under the most extreme conditions. As such, studying how their final stellar populations are assembled from their natal progenitor gas clouds can provide strong constraints on star formation theories. An obvious place to look for the initial conditions of such extreme stellar clusters is gas clouds of comparable mass and density, with no star formation activity. We present a method to identify such progenitor gas clouds and demonstrate the technique for the gas in the inner few hundred pc of our Galaxy. The method highlights three clouds in the region with similar global physical properties to the previously identified extreme cloud, G0.253 + 0.016, as potential young massive cluster (YMC) precursors. The fact that four potential YMC progenitor clouds have been identified in the inner 100 pc of the Galaxy, but no clouds with similar properties have been found in the whole first quadrant despite extensive observational efforts, has implications for cluster formation/destruction rates across the Galaxy. We put forward a scenario to explain how such dense gas clouds can arise in the Galactic Centre environment, in which YMC formation is triggered by gas streams passing close to the minimum of the global Galactic gravitational potential at the location of the central supermassive black hole, Sgr A*. If this triggering mechanism can be verified, we can use the known time interval since closest approach to Sgr A* to study the physics of stellar mass assembly in an extreme environment as a function of *absolute time*.

Key words: stars: early-type – stars: formation – ISM: clouds – ISM: evolution – Galaxy: centre – galaxies: star clusters: general.

1 INTRODUCTION

Stars in the most massive and dense stellar clusters must form at high protostellar densities and in close proximity to large numbers of high-mass stars. The dynamical interactions and (proto)stellar feedback they experience make this one of the most extreme environments in which stars can form. The progenitor clouds of these super star clusters therefore provide an ideal laboratory for understanding how environmental conditions affect the physics governing star formation.

The inner few hundred parsecs of the Milky Way – the ‘Central Molecular Zone’ (CMZ) – is an ideal location in the

Galaxy to search for molecular cloud progenitors of the most massive ($>10^4$ – $10^5 M_{\odot}$) and dense (radius ~ 1 pc) stellar clusters [often called young massive clusters (YMCs); see Portegies Zwart, McMillan & Gieles 2010. The CMZ holds a substantial molecular gas reservoir of 2 – $7 \times 10^7 M_{\odot}$ (Morris & Serabyn 1996; Ferrière, Gillard & Jean 2007) which has an average volume density two orders of magnitude larger than that in the disc, and it has been known for several decades that parts of this gas reservoir contain very cold, dense cores with little signs of star formation activity (e.g. the ‘dust ridge’; Lis et al. 1994, 1999, 2001; Lis & Menten 1998).

Several studies have highlighted one CMZ molecular cloud in particular – variously known as M0.25, G0.253 + 0.016, the Brick or the Lima Bean – as extreme and potentially representing the initial conditions of a YMC (Lis & Menten 1998; Lis et al. 2001;

*E-mail: s.n.longmore@ljmu.ac.uk

Bally et al. 2010; Longmore et al. 2012). In retrospect, G0.253 + 0.016 was easy to identify because it is so bright and isolated in the far-IR/sub-mm emission maps, and stands out so clearly as an IR absorption feature. However, G0.253 + 0.016 contains less than one hundredth of the total mass of the CMZ. It is therefore possible that other, less conspicuous, YMC progenitor clouds may exist but have not yet been identified as such in previous work. In this Letter, we return to the same data that Longmore et al. (2012) used to identify and characterize G0.253 + 0.016, but now attempt a more systematic approach to finding YMC progenitor clouds in the CMZ.

2 IDENTIFYING MOLECULAR CLOUD PRECURSORS OF BOUND YMCs IN THE GALACTIC CENTRE

Most lines of sight along the Galactic plane contain substantial emission from gas at varying distances. However, the vast majority of the far-IR and sub-mm continuum emission within $|l| \sim 1^\circ$ is from molecular gas at the Galactic Centre (GC) distance (Morris & Serabyn 1996; Molinari, Bally & Noriega-Crespo 2011). Uniform angular resolution then relates directly to a uniform physical resolution, and uniform flux sensitivity corresponds to a roughly uniform mass sensitivity. Under these circumstances, it is then possible to calculate the total mass as a function of radius from any given pixel in a column density map, and use this to identify YMC progenitor clouds.

However, from the column density map alone, it is not possible to tell how much of the mass within that radius is physically associated – i.e. there is no guarantee that the projected distance in the plane of the sky bears any relation to the physical separation between two points. Also, given the complicated velocity structure in the CMZ, a single pixel may contain flux contributions from multiple, physically distinct components along the line of sight. However, this is easily identified by referring to molecular line data where the additional velocity information uncovers the gas kinematic structure.

Even if the gas kinematics shows that the emission at one spatial position is from a single object, it is possible that the object may be significantly more extended along the line of sight than inferred from the projected radius in the plane of the sky. The average volume density would therefore be lower than that assuming spherical symmetry. It is possible, for instance, that high column density peaks observed towards the GC may be elongated filaments (like those seen in the barred spiral galaxy NGC 1097) seen end-on. We use the threshold volume density, n_{thresh} , required for gas clouds to overcome the extreme tidal forces at a distance R_{GC} from the GC ($n_{\text{thresh}} > 10^4 \text{ cm}^{-3} \times (75 \text{ pc}/R_{\text{GC}})^{1.8}$; Guesten & Downes 1980) to estimate the extent of clouds along the line of sight. For clouds at representative distances from the GC of 50 and 100 pc (Ferrière et al. 2007; Molinari et al. 2011), this implies a maximum radius for spherical gas clouds massive enough to form YMCs ($\sim 10^5 M_\odot$) of approximately 1–3 pc. By choosing these projected radii limits to define the ‘enclosed mass’ below, any gas clouds must have a similar extent along the line of sight as they do in the plane of the sky, otherwise they would quickly be shredded into tenuous gas.

Bressert et al. (2012, hereafter B12) propose that bound YMCs form from massive ($\gtrsim 10^5 M_\odot$) clouds enclosed within a sufficiently small radius that the escape speed exceeds the sound speed in photoionized gas. These criteria infer an additional criterion of the minimum mass as a function of radius required for a gas cloud to proceed to form a bound YMC.

Using the Herschel Galactic Plane Survey (HiGAL) column density map as a measure of the spatial distribution of mass (Molinari et al. 2011), and H₂O Galactic Plane Survey (HOPS) molecular line

data to resolve the kinematic structure (Walsh et al. 2011; Purcell et al. 2012), we now aim to assess which parts of the CMZ pass the B12 criteria, and hence identify candidate YMC progenitor clouds.

We do this on a pixel-by-pixel basis across the column density map by calculating the mass enclosed within a given projected radius on the plane of the sky. The top and bottom panels of Fig. 1 show the resulting ‘enclosed-mass’ map for a projected radius of 1 and 3 pc, respectively. The colour scale reflects the mass range, the magnitude of which is given by the colour bar on the right-hand edge of the panel. The lowest (black) contour levels in each panel show the approximate threshold mass within 1 pc (top) and 3 pc (bottom) that B12 predict should form a bound YMC. The regions enclosed within these contours are initial candidate YMC progenitor clouds.

The top panel of Fig. 1 contains annotations identifying each of the candidate YMC progenitor clouds. The locations of the central, supermassive black hole, Sgr A*, and the Arches and Quintuplet clusters are also shown for orientation. This area of the Galaxy has been studied intensively, so these sources are generally well known (see Morris & Serabyn 1996). Sgr B2 and Sgr C host H II regions, and Sgr B2’s high star formation rate means it is often referred to as a mini-starburst. The 20 and 50 km s⁻¹ clouds lie closest in projection to the supermassive black hole, Sgr A*, and it has been suggested that they are currently being tidally disrupted by a close interaction (Herrnstein & Ho 2005). G0.253 + 0.016 and clouds ‘d’, ‘e’ and ‘f’ are well-studied, sub-mm-bright sources in the so-called dust ridge (see Lis et al. 1994; Lis & Menten 1998; Immer, Menten & Schuller 2012 for details).

The 1 pc enclosed-mass map (top panel of Fig. 1) shows one candidate source close to the B12 limit which is not a well-known object, at $(l, b) \sim (-0.39, -0.25)$. This is easy to identify in the HOPS NH₃(1, 1) data cubes as a foreground cloud, by the much narrower linewidth (a few km s⁻¹) compared to the rest of the clouds in the CMZ. The mass determined from the column density map assuming a GC distance is therefore an overestimate. We remove this source from the list of candidate YMC precursors.

The other candidate at $(l, b) \sim (0.1, -0.05)$ shows only a single velocity component at this position in the HOPS NH₃(1, 1) data, and the broad linewidth is consistent with this gas lying at the GC distance. While this candidate is close to the B12 criteria at an enclosed-mass radius of 1 pc (top panel of Fig. 1), it is not above the B12 criteria at an enclosed-mass radius of 3 pc (bottom panel of Fig. 1). We therefore do not include this as a robust candidate YMC precursor cloud in further analysis. A similar argument holds for Sgr C. The 20 and 50 km s⁻¹ clouds are likely to be distinct physical objects, but their close passage to Sgr A* makes their dynamical state uncertain, so we do not include them as YMC precursor candidates. Sgr B2 is known to have a complex kinematic structure with multiple velocity components as a function of position and several distinct and physically separated star formation regions (see Qin et al. 2011, and references therein). The assumptions used to calculate the enclosed mass in Fig. 1 therefore do not hold for this region.

This leaves G0.253 + 0.016 – a previously identified YMC progenitor – and clouds ‘d’, ‘e’ and ‘f’. Immer et al. (2012) derive the detailed properties of clouds ‘d’, ‘e’ and ‘f’. They have masses of 7.2, 15.3 and $7.2 \times 10^4 M_\odot$, and radii of 3.5, 4.5 and 2.7 pc, respectively. HOPS NH₃(1, 1) data show that they have very similar integrated line profiles to G0.253 + 0.016, and virial analysis shows them to be close to gravitational stability. As a final check, we independently searched the Australia Telescope Compact Array (ATCA) NH₃ GC survey data (Ott et al., in preparation) and confirmed these sources as bright, isolated, compact, dense gas peaks with a single velocity component at higher angular resolution.

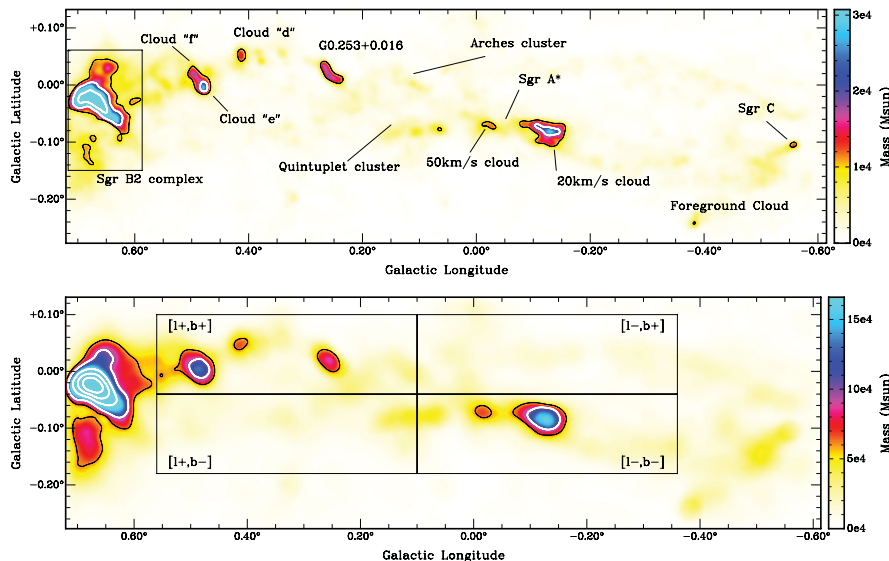


Figure 1. Maps of the ‘enclosed mass’ as a function of projected radius for the 100 pc ring orbiting the centre of the Milky Way. Every pixel in the image shows the mass within a projected physical radius of 1 pc (top) and 3 pc (bottom) of that pixel, derived from the HiGAL column density map of the region (Battersby et al. 2011; Molinari et al. 2011). The contours in the top image are at an enclosed mass within 1 pc of 1, 2 and $5 \times 10^4 M_{\odot}$. The contours in the bottom image are at an enclosed mass within 3 pc of 1, 2, 3, 4 and $5 \times 10^5 M_{\odot}$. The scale bar in the right-hand panel shows the linear mass colour stretch. The lowest contours in each panel, shown in black rather than white, correspond roughly to the mass versus radius criteria in B12 required for a gas cloud to form a bound YMC.

In summary, we reconfirm G0.253 + 0.016 as a potential YMC progenitor cloud using this method and highlight three other clouds (‘d’, ‘e’ and ‘f’) which also pass the B12 criteria.

3 IMPLICATIONS FOR YMC FORMATION

Further observations to derive the detailed gas properties of each cloud are required to determine if these candidate progenitors will form a YMC. In particular, observations¹ are needed to determine if the assumption of approximately spherical clouds is valid. This may not be the case. Dust structures and lanes in circum-nuclear gas rings of galaxies often show filamentary ‘streamers’ (see e.g. Peebles & Martini 2006). If such streamers exist in our own Galaxy, and they have orientations similar to those in external galaxies, one would expect to find them ‘end-on’ to our line of sight in the receding velocity part of the first quadrant. This is where we find all the highest column density gas and candidate YMC progenitor clouds. If some of these are filamentary streamers, they may be on the verge of being sheared by tides – a natural explanation of their lack of star formation (see e.g. Kauffmann, Pillai & Zhang 2013).

However, we know that YMCs form in this part of the Galaxy, so we should also expect to find precursor clouds. The clouds mentioned above are the best candidates for the initial conditions of future Arches-like stellar clusters. Therefore, it seems reasonable to assume that at least one of these will proceed to form such a cluster.

If YMCs all form in a similar way from clouds with similar initial conditions, comparing the number of clouds at the same evolutionary stages in different locations provides a direct comparison of the YMC formation rate between the regions. Therefore, the fact that Ginsburg, Bressert & Bally (2012) find no starless YMC progenitor clouds with similar mass and density in the first quadrant of the Galaxy ($6^{\circ} < l < 90^{\circ}$, $|b| < 0.5$) implies that more YMCs are currently forming per unit time in the GC than the disc. For the

ISM conditions in the inner few hundred pc of the GC, Kruijssen (2012) predicts that a much higher fraction (~ 50 per cent) of stars will form in gravitationally bound stellar clusters compared to the local solar neighbourhood (~ 7 per cent). So per unit star formation rate the CMZ should be much more efficient at forming bound clusters. However, YMCs show no preferred galactocentric radius in any galaxy, including the Milky Way (Portegies Zwart et al. 2010). Reconciling these facts would require that the YMCs forming in the centre of the Milky Way have correspondingly shorter lifetimes after formation than elsewhere in the Galaxy. Simulations suggest that this is the case (e.g. Portegies Zwart et al. 2001; Kruijssen, Pelupessy & Lamers 2011). In the central 300 pc of their model galaxy, Kruijssen et al. (2011) find that the disruption time is at least an order of magnitude shorter than in the disc. These model predictions are consistent with the large number of observed progenitor molecular clouds in the CMZ compared to the rest of the Galaxy but no correspondingly large number of long-lived YMCs. In this scenario, while more are being created, they are also being destroyed at a higher rate, so at any given snapshot in time the YMC number density does not vary with galactocentric radius.

Another possibility is that the formation mechanism for YMCs outside the GC is different. Rather than forming in a short burst from the prompt collapse of such dense gas clouds, YMCs may form over an extended period much longer than the free-fall time, via continuous accretion (e.g. Smith, Longmore & Bonnell 2009). In this case, one would not expect to see G0.253 + 0.016-like clouds in the Galactic disc. The implications of this – that YMC formation mechanisms vary with environment – has important consequences for interpreting observed YMC distributions in external galaxies.

3.1 YMC formation triggered by gas interacting with the gravitational potential around Sgr A*

In an attempt to distinguish between these possibilities, we now try to understand how the CMZ environment may be playing a role in

¹ For example, direct volume density measurements (e.g. Ginsburg et al. 2011) or comparison to numerical models (e.g. Clark et al. 2013).

Table 1. Properties of the four equal-area regions discussed in the text and illustrated in the bottom panel of Fig. 1.

Region	l_{\min} ($^{\circ}$)	l_{\max} ($^{\circ}$)	b_{\min} ($^{\circ}$)	b_{\max} ($^{\circ}$)	Mass ($10^5 M_{\odot}$)
$[l+, b+]$	0.1	0.56	-0.04	0.1	11.9
$[l+, b-]$	0.1	0.56	-0.18	-0.04	6.1
$[l-, b+]$	-0.36	0.1	-0.04	0.1	5.6
$[l-, b-]$	-0.36	0.1	-0.18	-0.04	11.2

creating such massive and dense molecular clouds that appear to be about to form YMCs.

We note that the distribution of the *densest* gas in Fig. 1 is asymmetric. The potential YMC progenitor clouds lie at positive latitudes between roughly Sgr A* and Sgr B2. To see if this asymmetry in gas density is reflected in the distribution of total mass, we broke up the region into four rectangular segments of equal area, split at half the projected distance between Sgr B2 and Sgr C. We discarded Sgr B2 and Sgr C themselves due to saturation and potential line-of-sight issues. The l and b ranges of the four areas are listed in Table 1, and shown in the bottom panel of Fig. 1. The final column in Table 1 shows the total mass in each of the four quadrants, which all agree to within a factor of 2. The increased density in the $[l+, b+]$ quadrant is not simply due to a higher total mass.

We then seek an explanation for what might be causing the increased gas density. In order to do this, we need to make some assumptions about the 3D geometry of the gas. Molinari et al. (2011) recently proposed that the molecular gas within $\sim 1^{\circ}$ of the GC lies in a ring orbiting the GC. An interesting aspect of this model is that the supermassive black hole, Sgr A*, is not at the geometric centre. Instead, it is closer to the front side of the ring. As Fig. 2 shows, the gas therefore passes close to the bottom of the Galactic gravitational potential as it orbits from Sgr C to Sgr B2. It seems reasonable to assume that the gas may have been affected by the varying gravitational potential along this orbit, with the strongest effect at pericentre passage. Note that the location of Sgr A* relative to the gas is important in as far as it represents the bottom of the Galactic gravitational potential. However, Sgr A*'s radius of gravitational influence is $\lesssim 2$ pc. Therefore, given plausible gas

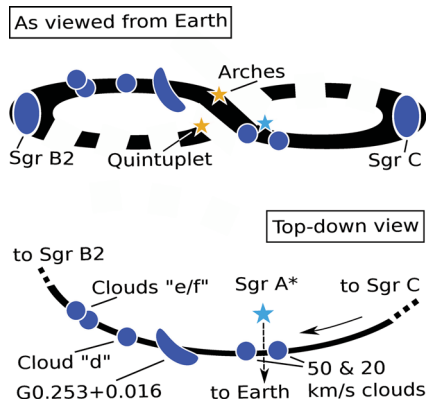


Figure 2. Upper: schematic diagram of the gas in the inner $\sim 1^{\circ}$ of the Galaxy as viewed from Earth. The thick solid and dashed black lines represent the stream of gas moving from Sgr C to Sgr B2 and the far side of the ring, respectively, in the Molinari et al. (2011) model. Lower: top-down view of this gas stream. The curved arrow shows the sense of rotation. Between Sgr C and Sgr B2 the gas passes close to the bottom of the Galactic gravitational potential denoted by the supermassive black hole, Sgr A*. The upper and lower parts are approximately aligned vertically.

trajectories, the gravitational field felt by the gas is likely to be dominated instead either by the nuclear cluster surrounding Sgr A* or the nuclear stellar disc, which are the main contributors to the potential at radii of 2–30 and 30–300 pc, respectively (Launhardt, Zylka & Mezger 2002).

Gas moving on an orbit around a source of strong gravitational potential will feel a combination of two effects as it approaches pericentre. First, it will experience increasing compression in the vertical direction perpendicular to the orbit. At the same time, it will also become more stretched along the orbit. It is interesting to note in this regard that G0.253 + 0.016, a cloud in this scenario that recently passed through pericentre to the bottom of the Galactic potential, appears extended along the orbit proposed by Molinari et al. (2011) and has a small scaleheight compared to the majority of the gas in the ring.

The fate of the gas after pericentre passage will depend on many factors. We are currently investigating this scenario numerically, paying particular attention to understanding the phase space distribution of the gas (Kruijssen et al., in preparation) and comparing this directly to observations (Rathborne et al., in preparation).

In this scenario, one interpretation of the density contrast of gas up and downstream from pericentre passage is that the net effect of the interaction is a compression of the gas. We speculate that this is aided by the gas dissipating the tidally injected energy, which would be observable as strongly shocked gas. A direct prediction of this is that the hydrodynamic shocks should be strongest around pericentre passage than elsewhere in the region.

How might the interaction with the bottom of the Galactic gravitational potential affect the star formation activity? Given the reservoir of dense gas available to form stars, the gas in the inner few hundred pc of the Galaxy is known to be underproducing stars by at least an order of magnitude compared to commonly assumed star formation relations (Longmore et al. 2013). So if the gas was previously sitting close to gravitational stability, the additional net compression of the gas might be enough for it to begin collapsing to form stars. With this scenario in mind, it is interesting to note that the YMC progenitor clouds progressively farther downstream from pericentre passage with Sgr A* show progressively more star formation activity. The closest cloud downstream, G0.253 + 0.016, shows little signs of star formation activity (e.g. Longmore et al. 2012; Kauffmann et al. 2013; Rodriguez & Zapata 2013). Cloud ‘d’ has methanol maser emission; signposting massive star formation is underway (Immer et al. 2012). As mentioned above, Sgr B2 has prodigious star formation activity.

Further observations are required to test this tentative evolution of star formation activity from Sgr A* to Sgr B2. However, if the hypothesis proves correct, the implications are potentially exciting. Given the observed orbital velocity of the gas, we can calculate the time since each of the clouds passed pericentre, i.e. the time at which star formation may have been instigated. Assuming an orbital velocity of 80 km s^{-1} (Molinari et al. 2011), the projected distances of G0.253 + 0.016, cloud ‘d’ and clouds ‘e/f’ from Sgr A* suggest they passed pericentre approximately 0.6, 0.9 and 1.0 Myr ago, respectively. Therefore, we may have a truly unique opportunity to effectively follow the physics shaping the formation of the most massive stellar clusters in the Galaxy, and by inference the next generation of the most massive stars in the Galaxy, as a function of *absolute* time.

An additional prediction of this scenario is that the resulting stellar clusters should have kinematics consistent with their having formed from gas on this orbital trajectory. As shown in Fig. 2, the two known YMCs in the region – the Arches and Quintuplet

clusters – are observed to lie in projection along the ring. However, the cluster ages are comparable to the ring’s orbital period, so their current locations do not necessarily reflect where they formed. In addition, determining the true distance of these clusters from the GC and constraining their orbital properties are observationally challenging (Figer, McLean & Morris 1999; Figer et al. 2002; Stolte et al. 2008; Clarkson et al. 2012; Hußmann et al. 2012). While some observed properties (e.g. the cluster proper motions) are consistent with them having been associated with the gas in the ring, further work is needed to determine if the proposed scenario can explain the origin of the Arches and Quintuplet clusters.

We emphasize that the scenario outlined above depends on the model of Molinari et al. (2011) in only two ways. First, we assume that the gas moving from Sgr C to Sgr B2 is a coherent stream. Secondly, we assume that between these two points the gas passes close to the bottom of the Galactic gravitational potential. The scenario does not rely on other aspects of the Molinari et al. (2011) model, such as the rotation velocity, whether Sgr B2 is closer/farther from Earth than Sgr A* or whether Sgr B2/Sgr C are tangent points of the ring at the intersection of the x_1 and x_2 orbits.

3.2 Asymmetry in the total gas mass distribution

Returning to the values in Table 1, it is striking that the mass for the $[l+, b+]$ and $[l-, b-]$ quadrants agree so closely, as do the $[l+, b-]$ and $[l-, b+]$ quadrants. However, the masses of the former are a factor of 2 larger than the latter. Could this be the result of a systematic bias? The gas in this region is all thought to lie within ~ 100 pc of the GC (e.g. Ferrière et al. 2007; Molinari et al. 2011) so the distance dependence on the mass is at the $(\Delta\text{distance}/\text{distance})^2 \sim (100/8500)^2 \sim 10^{-4}$ level and hence can be neglected. While there may be mechanisms through which the dust properties may vary in the GC environment, it would be curious that such a disparity has not been noticed before in such a well-observed region. We note that the $[l+, b+]$ and $[l-, b-]$ quadrants and $[l+, b-]$ and $[l-, b+]$ quadrants encapsulate the near and far sides of the ring, respectively, in the Molinari et al. (2011) model. It is interesting to speculate whether the apparent factor of 2 decrease in gas mass on the far side of the ring may be either caused by changes in dust properties or gas leaving the ring due to star formation activity within Sgr B2. We flag this as an interesting avenue for further investigation.

4 CONCLUSIONS

We present a method for finding YMC progenitor clouds and use this to identify four candidate proto-YMC clouds in the inner few hundred pc of our Galaxy. We discuss the significance of finding four such YMC progenitor clouds with very little signs of star formation in such a small volume of the Galaxy, while no starless YMC progenitor clouds have been found in the first quadrant of the Galaxy. We infer that in environments like the GC, YMCs either form via a different mechanism or the formation and destruction times are much shorter. We then investigate the distribution of the gas and put forward a scenario to explain the observed asymmetry in the dense gas distribution. We propose that gas is compressed by passing close to the minimum of the global Galactic gravitational potential. We speculate that this may instigate the condensation of dense YMC progenitor clouds, which leads to the subsequent formation of stars towards Sgr B2. If this hypothesis can be verified, we may have a truly unique opportunity to effectively follow the physics shaping the formation of the most massive stellar clusters

in the Galaxy, and by inference the next generation of the most massive stars in the Galaxy, as a function of *absolute* time.

ACKNOWLEDGEMENTS

We would like to thank the anonymous referee for their prompt, positive and constructive comments. SNL would like to thank Henrik Beuther, Ian Bonnell, Jim Dale, Betsy Mills, Mark Morris and Malcolm Walsmley for insightful discussions. SNL acknowledges that this research has received funding from the European Community’s Seventh Framework Programme (FP7/2007-2013/) under grant agreement No 229517.

REFERENCES

- Bally J., Aguirre J., Battersby C., Bradley E. T., Cyganowski C., 2010, *ApJ*, 721, 137
- Battersby C., Bally J., Ginsburg A., Bernard J.-P., 2011, *A&A*, 535, A128
- Bressert E., Ginsburg A., Bally J., Battersby C., 2012, *ApJ*, 758, L28 (B12)
- Clark P. C., Glover S. C. O., Ragan S. E., Shetty R., Klessen R. S., 2013, *arXiv:e-prints*
- Clarkson W. I., Ghez A. M., Morris M. R., Lu J. R., Stolte A., McCrady N., Do T., Yelda S., 2012, *ApJ*, 751, 132
- Ferrière K., Gillard W., Jean P., 2007, *A&A*, 467, 611
- Figer D. F., McLean I. S., Morris M., 1999, *ApJ*, 514, 202
- Figer D. F. et al., 2002, *ApJ*, 581, 258
- Ginsburg A., Darling J., Battersby C., Zeiger B., Bally J., 2011, *ApJ*, 736, 149
- Ginsburg A., Bressert E., Bally J., 2012, *ApJ*, 758, L29
- Guesten R., Downes D., 1980, *A&A*, 87, 6
- Herrnstein R. M., Ho P. T. P., 2005, *ApJ*, 620, 287
- Hußmann B., Stolte A., Brandner W., Gennaro M., Liermann A., 2012, *A&A*, 540, A57
- Immer K., Menten K. M., Schuller F., 2012, *A&A*, 548, A120
- Kauffmann J., Pillai T., Zhang Q., 2013, *ApJ*, 765, L35
- Kruijssen J. M. D., 2012, *MNRAS*, 426, 3008
- Kruijssen J. M. D., Pelupessy F. I., Lamers H. J. G. L. M., 2011, *MNRAS*, 414, 1339
- Launhardt R., Zylka R., Mezger P. G., 2002, *A&A*, 384, 112
- Lis D. C., Menten K. M., 1998, *ApJ*, 507, 794
- Lis D. C., Menten K. M., Serabyn E., Zylka R., 1994, *ApJ*, 423, L39
- Lis D. C., Li Y., Dowell C. D., Menten K. M., 1999, in Cox P., Kessler M., eds, *ESA Special Publication, Vol. 427, Cold GMC Cores in the Galactic Centre*. ESA, Noordwijk, p. 627
- Lis D. C., Serabyn E., Zylka R., Li Y., 2001, *ApJ*, 550, 761
- Longmore S. N. et al., 2012, *ApJ*, 746, 117
- Longmore S. N., Bally J., Testi L., Purcell C. R., Walsh A. J., 2013, *MNRAS*, 429, 987
- Molinari S., Bally J., Noriega-Crespo A., 2011, *ApJ*, 735, L33
- Morris M., Serabyn E., 1996, *ARA&A*, 34, 645
- Peeples M. S., Martini P., 2006, *ApJ*, 652, 1097
- Portegies Zwart S. F., Makino J., McMillan S. L. W., Hut P., 2001, *ApJ*, 546, L101
- Portegies Zwart S. F., McMillan S. L. W., Gieles M., 2010, *ARA&A*, 48, 431
- Purcell C. R. et al., 2012, *MNRAS*, 426, 1972
- Qin S.-L., Schilke P., Rolffs R., Comito C., 2011, *A&A*, 530, L9
- Rodriguez L. F., Zapata L., 2013, *ApJ*, 767, L13
- Smith R. J., Longmore S., Bonnell I., 2009, *MNRAS*, 400, 1775
- Stolte A., Ghez A. M., Morris M., Lu J. R., Brandner W., Matthews K., 2008, *ApJ*, 675, 1278
- Walsh A. J. et al., 2011, *MNRAS*, 416, 1764